Chirped Phase Mask Interferometer for Fiber Bragg Grating Array Inscription

Martin Becker, Tino Elsmann, Ines Latka, Manfred Rothhardt, and Hartmut Bartelt

***Abstract*—We present a phase mask inscription technique with two beam interferometry using a lateral nonhomogeneous beam splitter to create gratings with nonhomogeneous periods, the so-called chirped fiber Bragg gratings. Inscription experiments with deep ultraviolet excimer and femtosecond laser sources reveal how this inscription method depends on the coherence properties of the inscription laser. Nonhomogeneous beam splitters are shown to provide a method to generate chirped fiber Bragg gratings with great wavelength versatility, even with the ultraviolet femtosecond laser.**

***Index Terms*—Femtosecond laser, fiber Bragg gratings, optical fiber filters, two-beam interferometry.**

I. Introduction

CONTINUOUSLY chirped fiber Bragg gratings (C-CFBG) are key components for dispersion compensation [1] and light source tailoring [2], [3], and are used as broad reflection bandwidth laser mirrors [4]. When dispersion properties do not matter, broad bandwidth reflection gratings can also be achieved with homogeneous index modulation profiles. In this case, the bandwidth is given by the superposition of the number of grating fringes and the applied refractive index increase [5]. For strong gratings, where the refractive index modulation increase Δn exceeds the inverse number of grating fringes N ($\Delta n/(2n_{\mathrm{eff}}) \gg 1/N$), the approximate full-width-half-maximum (FWHM) reflection bandwidth $\Delta\lambda_{\mathrm{Bragg}}$ can be described as

$$\Delta\lambda_{\mathrm{Bragg}} \approx \lambda_{\mathrm{Bragg}} \frac{\Delta n}{2n_{\mathrm{eff}}} \tag{1}$$

where n_{eff} is the effective refractive index of the wave guide. Experimentally, one observes that the nonlinear properties of photosensitivity, the limited interference contrast of the inscription laser, and a non-perfect beam stability lead to a decay of the refractive index modulation of the grating during inscription [6]–[8]. Therefore, chirped FBGs are required for many broadband filtering applications, especially with a well-tailored reflection wavelength.

Chirped gratings can be obtained with a chirped phase mask [9] and concatenated phase masks [10]. Chirped gratings have been implemented with a homogeneous phase mask using the phase mask moving technique [11], fiber tilting [12], tapered fiber structures [13]–[15], and stretching or bending the fiber during inscription with phase masks [16], [17]. For all these methods, the reflection wavelength and bandwidth remain closely connected to the choice of the applied phase mask.

Several attempts have been made to apply two beam interferometry to realize chirped gratings due to the great Bragg wavelength versatility of this method. One option is the use of consecutive subgratings made by continuously moving fringe patterns [18]–[22]. Another is the Sagnac interferometer with an integrated phase shifting element [23], [24], where chirp rates of 0.48 nm/cm are achieved. CFBGs with an interferometer setup were also realized through lenses placed inside of the interferometer arms [22], [25] or with the usage of a prism spectrometer [26].

As chirped gratings strongly depend on homogeneous sample exposure, continuous wave lasers are preferred [22]. But the emergence of ultrashort pulse lasers allows refractive index changes to be induced in materials that do not provide conventional photosensitivity [27], [28]. Therefore, adapted inscription methods are proposed which are compatible with ultrashort-pulse laser sources. A direct approach is by the phase mask inscription method with chirped phase masks [29]. Alternative approaches use phase masks with constant pitch and bent fibers [30], tilted wave fronts [31] or a PMMA phase mask together with a thermal gradient [32]. Point-by-point inscription has been demonstrated to be another candidate for CFBG inscription [33].

In this paper we analyze a method in which we integrate a chirped phase mask in an interferometer to realize a continuously chirped phase mask interferometer (C-CPMI) [34]. Two-beam interferometry [35], [36] offers various advantages: it provides wavelength versatility and it works free of contact. It provides a large distance between target fiber and the optical elements and allows high energy density at the fiber position without degradation of the optical components of the interferometer. It is suitable for inscription with ultraviolet and visible femtosecond laser exposure [37], [38]. Additionally, it allows gratings to be written on the fly during the fiber drawing process [39], [40]. The C-CPMI combines all these advantages with CFBG inscription. Additionally, it prevents Talbot diffraction patterns across the waveguide, as can be observed with phase mask inscription [41], [42].

Manuscript received November 6, 2014; revised January 8, 2015; accepted January 18, 2015. Date of publication January 19, 2015; date of current version March 16, 2015. This work was supported by the ERDF program and by the Thuringian Ministry of Education, Science and Culture. Experiments were conducted within the Fiber Health Probe under Grant 13N12525 and SiFas-P under Grant 13INE036 research initiatives of the German Federal Ministry of Education and Research (BMBF), and under Contract 2011 FGR 0104 (FG Faser-Tech) with the Thuringian Ministry of Economics, Labor and Technology.

The authors are with the Leibniz Institute of Photonic Technology, 07745 Jena, Germany (e-mail: martin.becker@ipht-jena.de; tino.elsmann@ipht-jena.de; ines.latka@ipht-jena.de; Manfred.Rothhardt@ipht-jena.de; hartmut.bartelt@ipht-jena.de).

Color versions of one or more of the figures in this paper are available online at http://ieeexplore.ieee.org.

Digital Object Identifier 10.1109/JLT.2015.2394299

This article has been accepted for publication in a future issue of this journal, but has not been fully edited. Content may change prior to final publication. Citation information: DOI 10.1109/JLT.2015.2394299, Journal of Lightwave Technology

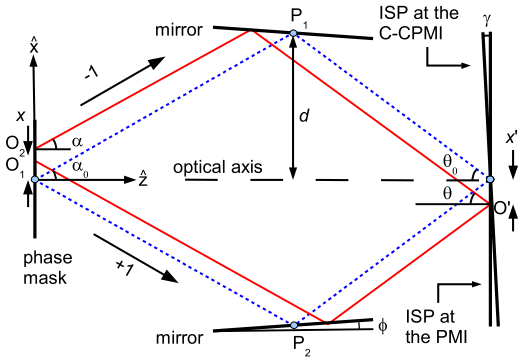

Fig. 1. Chirped PMI setup. At the C-CPMI, the ISP is not perpendicular to the optical axis but tilted at an angle γ. Interfering rays departing from the center of the phase mask (blue dashed line) and from the red side of the phase mask (red solid line) are included.

II. Theoretical Approach to the Interferometric Setup With Phase Mask

The phase mask interferometer (PMI) (see Fig. 1) splits an incoming ray at the beam-splitting phase mask into two rays with an angle α relative to the optical axis. This angle is defined by the period of the beam-splitting phase mask Λ_{PM} and the inscription wavelength λ_{inscr}. For the first diffraction orders ($m = \pm 1$) it is defined through the relation $\sin(\alpha) = \lambda_{\mathrm{inscr}}/\Lambda_{\mathrm{PM}}$. These rays are then directed to the fiber position at an angle θ and provide a standing wave pattern along the fiber axis. Assuming that the fiber provides photosensitivity and interacts with the light of the inscription laser, then the interaction of the light with the waveguide results in a grating with center reflection wavelength of

$$\lambda_{\mathrm{Bragg}} = n_{\mathrm{eff}} \frac{\lambda_{\mathrm{inscr}}}{\sin\theta} \tag{2}$$

where $\theta = \alpha + 2\phi$ defines the angle of the rays crossing the fiber in relation to the optical axis, and ϕ is the tilt angle between the mirrors and the *xy*-plane. The tilt direction of the mirrors is symmetrical to the optical axis. In a non-chirped PMI, the fiber is placed inside the ideal sample plane (ISP). This plane is perpendicular to the optical axis and its distance from the phase mask is defined by

$$z_{\mathrm{ISP}} = d\left(\tan^{-1}(\alpha) + \tan^{-1}(\theta)\right) \tag{3}$$

where d is the distance between the pivot points (P_1 and P_2) of the mirrors and the optical axis, which is assumed be the same for both mirrors. The interferometer has two scaling factors: the magnification factor S_{M} and the wavelength scaling factor S_{W}. The first one defines the magnfication of the PMI [37]:

$$S_{\mathrm{M}} = \frac{x'}{x} = \frac{\cos(\alpha_0)}{\cos(\theta_0)}. \tag{4}$$

Here, x' marks a corresponding position on the sample plane. The wavelength scaling factor S_{W} defines the relation between the central period of the beam splitter and the resulting Bragg reflection wavelength:

$$S_{\mathrm{W}} = \frac{\lambda_{\mathrm{Bragg}}}{n_{\mathrm{eff}}\Lambda_0} = \frac{\sin(\alpha_0)}{\sin(\theta_0)}. \tag{5}$$

A. Calculation of the Chirp

The presented approach for the interferometric inscription setup uses a continuously chirped phased mask as a beam-splitter. The direct consequence is that the diffraction angle $\alpha(x)$ depends on the incoming position x of the rays at the phase mask. This results in an angular distribution of the interfering rays at the fiber position and consequently forms a continuously chirped interference pattern. The linear chirped phase mask is described by the chirp parameter σ which is defined as [43]

$$\frac{1}{\Lambda}(x) = \frac{1}{\Lambda_0}\left(1 + \sigma\frac{x}{L}\right) \tag{6}$$

where L is the length of phase mask, Λ_0 is the center period of the phase mask, and x marks a specific position on the phase mask. The overall chirp range of the whole phase mask is calculated to be approximately $\Delta\Lambda = \sigma\Lambda_0$. Note that $\Lambda_0\sigma/L$ is the chirp rate of the phase mask, usually given in nm/cm. The change of the diffraction angle $\alpha(x)$ with incoming beam position at the phase mask is

$$\sin\left(\alpha(x)\right) = \left(1 + \frac{\sigma}{L}x\right)\sin\alpha_0 \tag{7}$$

where α_0 is the reference angle $\sin\alpha_0 = \lambda_{\mathrm{inscr}}/\Lambda_0$.

It is important to define the orientation of the ISP for the C-CPMI. This is the plane where all rays departing from the phase mask interfere. It is tilted by an angle γ with respect to the ISP of the standard-PMI. This tilt angle is derived from the variation of interference position (see equation (3)) at different positions x of the split rays at the phase mask:

$$\tan\gamma = \frac{\Delta z_{\mathrm{ISP}}}{S_{\mathrm{M}}\Delta x} = \frac{\sigma}{L}\frac{d}{\sin(\alpha)\cos(\alpha)S_{\mathrm{M}}}\left(1 + S_{\mathrm{W}}^2\right). \tag{8}$$

The tilt angle γ is zero for the standing wave condition ($\theta = 90°$) and $90°$ when the ISP is at infinity ($\theta = 0°$). Therefore, the ISPs for the C-CPMI and the PMI get closer for larger beam anges θ. The angle γ becomes zero also if the phase mask has no chirp.

The bandwidth of the chirped grating inscribed in the waveguide is derived from the dependence of the reflection wavelength (see equation (2)) and from the position of the incoming light at the beam-splitting phase mask defined by equation (7):

$$\Delta\lambda_{\mathrm{Bragg}} = n_{\mathrm{eff}}\, x_{\mathrm{E}}\frac{\Lambda_0\sigma}{L}\frac{S_{\mathrm{W}}^2}{S_{\mathrm{M}}}. \tag{9}$$

Here the value x_{E} is introduced. It defines the effective length of the exposed area at the phase mask. This value is limited by the size of the phase mask $|x_{\mathrm{E}}| \leq L/2$. The spectral reflection bandwidth allows calculation of the dispersion D, taken from reference [44], together with equation (9):

$$D = \frac{2S_{\mathrm{M}}^2}{\Lambda_0\frac{\sigma}{L}S_{\mathrm{W}}^2 c} \tag{10}$$

where c is the speed of light in vacuum. The phase-mask equivalent chirp rate at the fiber position can be derived from equation

This article has been accepted for publication in a future issue of this journal, but has not been fully edited. Content may change prior to final publication. Citation information: DOI 10.1109/JLT.2015.2394299, Journal of Lightwave Technology

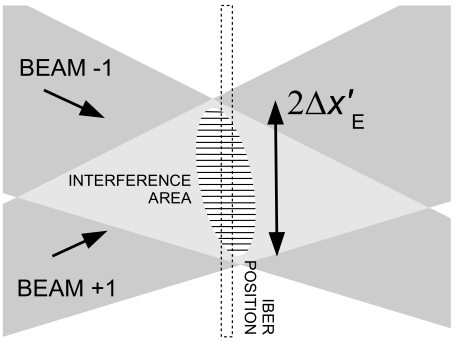

Fig. 2. Diamond-shaped overlap region for the C-CPMI. The interference area is tilted. One beam is slightly convergent and the other divergent. The length of the overlap x'_{E} is scaled to the effective length of the exposed area at the phase mask with equation (4).

(10) to be

$$\frac{\Delta\Lambda_{\mathrm{equiv}}}{\Delta x'} = \frac{2}{cD} = \frac{\Lambda_0\sigma}{L}\frac{S_{\mathrm{W}}^2}{S_{\mathrm{M}}^2} \quad .$$

B. Influence of the Coherence Properties of the Inscription Laser

The maximum effective length of a chirped fiber Bragg grating and, therefore, the grating reflection bandwidth depend on the size of the diamond-shaped overlap of the interfering beams at the ISP as shown in Fig. 2. This extent of potential interference is reduced due to the temporal and spatial coherence properties of the inscription laser [37].

In our experiments, we placed the fiber perpendicularly to the optical axis at the distance calculated with equation (3). This was done to prevent tilted FBG-fringes and to avoid coupling of guided light from the core into the cladding [45]. The focal length of the phase mask $f = \pm\sigma\tan(\alpha)/L$ (see Fig. 2) also defines the tilt angle of the interference fringes according to the standing wave condition. For the applied phase mask f is approximately 9 m. Therefore we expect that the induced tilt angles of the fringes itself are very small compared to the tilt of the interference pattern.

In the case where the fiber has no tilt angle, two rays interfering at the fiber originate from different positions on the phase mask (O_1 and O_2), except on the optical axis ($x = 0$), where these points coincide. The corresponding distance l_x of interfering rays departing from positions on the phase mask is defined by

$$l_x = \overline{O_1O_2} = 2 \times \Delta z_{\mathrm{ISP}}\frac{\sin\theta}{\cos\alpha} = 2x\tan\gamma\tan\theta \qquad (11)$$

where x is the distance in the phase mask position from the optical axis. It is at the center between the two points O_1 and O_2. When the value for l_x exceeds the spatial coherence length of the laser, the interference in the inscription plane ceases to exist. This is a direct consequence of the tilt of the interference at the ISP and is relevant for lasers with limited spatial coherence length.

TABLE I
LASERS USED FOR TESTING THE C-CPMI

Type	Excimer laser	Femtosecond laser
Wavelength	248 nm	267 nm
Pulse length	20 ns	400 fs
Pulse energy	150 mJ	0.3 mJ
Rep. rate	10 Hz	1000 Hz
Spat. coherence	450 μm	several millimeter
Temp. coherence	several millimeter	120 μm

The parameters given are experimentally applied values for FBG inscription.

For lasers with a short temporal coherence length, the maximum length l_t of a grating is given by [37]

$$l_t = \left|\frac{l_c^t\cos(\alpha)}{\sin(2\phi)}\right| \qquad (12)$$

where l_c^t is the temporal coherence length of the inscription laser. For small mirror tilt angles, this value is limited by the effective length of the exposed area on the phase mask. For $l_t < x_{\mathrm{E}}$ the spectral width is then limited by l_t according to equation (9) with the scaling factors (S_{M} and S_{W}) of unity: $\Delta\lambda_{\mathrm{Bragg}} = n_{\mathrm{eff}}\sigma\Lambda l_t/L$.

III. EXPERIMENTAL DETAILS

Inscription experiments with the C-CPMI are done with a phase mask fabricated in-house (IPHT) with a central pitch of 706.5 nm and a chirp rate of 2.3 nm/cm. The phase mask was manufactured using electron beam lithography [46].

For inscription experiments, two laser systems were used. Both systems provide high output power and high photon energy (deep ultraviolet, DUV), but with different coherence properties. One laser is the Mantis-Legend Elite-Tripler femtosecond laser from Coherent Inc. The other laser tested is a Compex 150 T KrF excimer laser from Lambda Physics, now Coherent. The operating parameters of the lasers used for experiments are listed in Table I.

A. Experimental Measurement of the Tilt Angle

To confirm the predicted values for the tilt angle γ as described by equation (8), we exposed the phase mask pointwise with a pin hole at two well-defined different positions at the *x*-axis. We then measured the resulting change of the overlap position of the rays using a high-precision translation stage to move a screen along the optical (*z*-)axis around the distance from the phase-mask according to equation (3) to find the intersection of the beams at the fiber position. This experiment was done for two mirror tilt positions and in comparison with a different phase mask (708.6 nm central period and 6.1 nm/cm chirp rate from Ibsen Photonics). The results are given in Fig. 3 and are compared with the expected values from equation (8). As predicted, the tilt angle γ increases with increasing chirp. It also increases with decreasing tilt angle of the mirrors and therefore with increasing Bragg reflection wavelength.

This article has been accepted for publication in a future issue of this journal, but has not been fully edited. Content may change prior to final publication. Citation information: DOI 10.1109/JLT.2015.2394299, Journal of Lightwave Technology

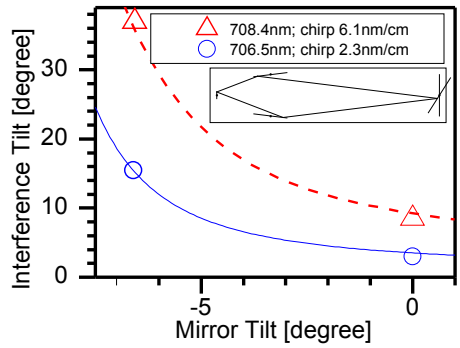

Fig. 3. Experimentally determined ISP tilt angles (circle, triangle) compared to theoretical prediction from equation (8) (lines). The inset shows the geometry of Fig. 1 and a tilt angle of $\phi = -7°$.

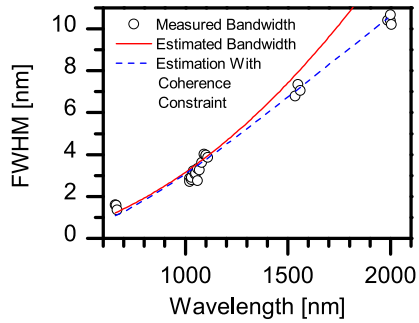

Fig. 5. Reflection bandwidth of the chirped gratings inscribed with excimer laser from the visible to the infrared. It increases with the target wavelength. At reflection wavelengths in the infrared, influence of the spatial coherence length becomes observable.

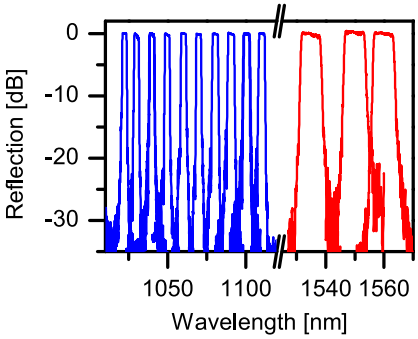

Fig. 4. Sample spectra of ten chirped gratings in the ytterbium amplification band and three chirped gratings in the erbium amplification band.

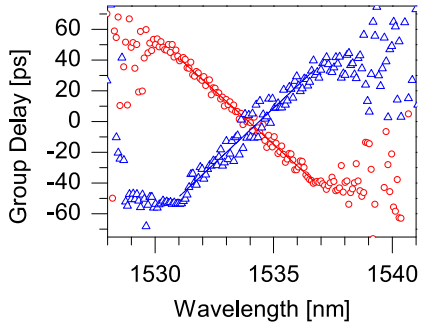

Fig. 6. Measured group delay of a chirped grating in both directions. Triangles are measured from blue to red, and circles *vice versa*.

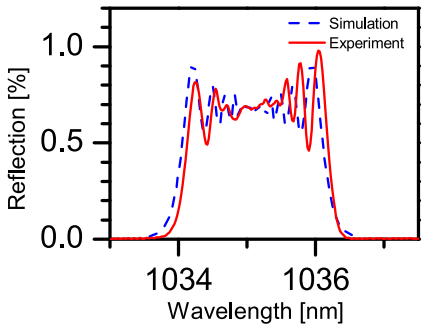

Fig. 7. Reflection spectrum of a single-pulse C-CFBG in a photosensitive fiber in comparison to theory.

B. *Inscription with Excimer Laser*

1) Chirped Multi-Pulse Gratings: We performed grating inscription experiments with the aforementioned phase mask from IPHT and an entrance slit of 1 cm to investigate the influence of the spatial coherence properties of the excimer laser. With this phase mask it was possible to inscribe chirped gratings from the visible spectral region (660 nm) up to the infrared (2000 nm). All gratings are inscribed in hydrogen-loaded commercial single-mode fibers (HP630, and 1060XP from Thorlabs Inc.,) [47], [48]. For the gratings that reflect in the short-wave infrared region (Er-Tm-band) we used a standard single-mode fiber following ITU-T G.652.

Sample spectra of grating arrays in the ytterbium and erbium amplification band are shown in Fig. 4. The reflection bandwidths of the resulting single grating increase with increasing wavelength from 3 nm at 1030 nm reflection bandwidth to 7 nm at 1550 nm. This behavior complies with observations in the literature, where longer reflection wavelengths come with broader reflection bandwidths [34]. The reflection bandwidth versus Bragg reflection wavelength is shown in Fig. 5. The estimated bandwidth using equation (9) (solid line) is also included. The dashed line in the same figure takes into account that the effective grating length is influenced by the spatial coherence length of the laser according to equation (11). Besides the bandwidth, we also measured the group delay of the grating at 1535 nm wavelength (see Fig. 4) using an optical network analyzer (Advantest Q7750 Optscope). The slope of the curves is shown in Fig. 6 and gives an experimental dispersion value of 14.2 ps/nm, which is close to the theoretically predicted value of 12.0 ps/nm according to equation (10).

2) Chirped Single-Pulse Gratings: Single-pulse fiber Bragg gratings are of great interest for situations where multiple pulses cannot be used for inscription. This applies especially for gratings written on the fly during the fiber drawing process [39], [40]. Fig. 7 shows the reflection spectrum of a grating written with a single pulse and a slit width of 7 mm. The fiber used is a single-mode photosensitive fiber with a highly germanium-doped core with about 18 mol% GeO_2. For comparison, the same figure

This article has been accepted for publication in a future issue of this journal, but has not been fully edited. Content may change prior to final publication. Citation information: DOI 10.1109/JLT.2015.2394299, Journal of Lightwave Technology

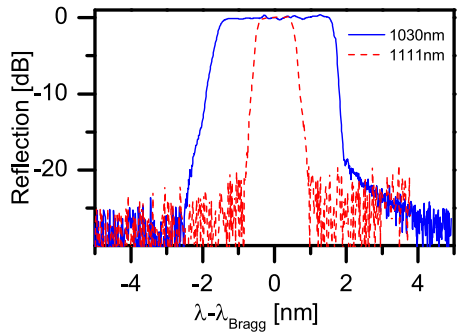

Fig. 8. Comparison of grating spectra made with femtosecond DUV radiation and different tilt angles of the mirrors. The reflection wavelengths are 1030 and 1111 nm respectively.

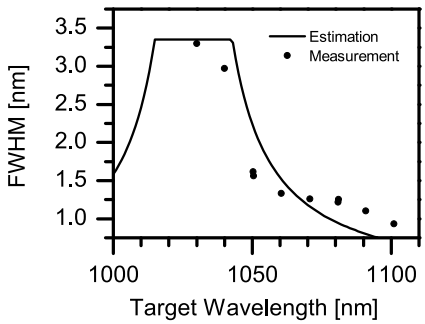

Fig. 9. Spectral width versus wavelength for FBG inscription with C-CPMI and DUV femtosecond laser. The solid line is an estimation for the spectral width to be achieved with the applied femtosecond laser. The dots are experimental values for the 3 dB reflection bandwidth.

includes the theoretical spectrum for a grating with 7 mm length and a refractive index modulation of $\Delta n = 2.6 \times 10^{-5}$, which was fitted with a transfer-matrix formalism [15], [49]. It shows a good agreement with the measured spectrum.

C. C-CFBG Array Inscription with DUV Femtosecond-Laser-Driven Interferometer

Fiber Bragg gratings are written with different reflection wavelengths in a single-mode fiber (1060XP) without hydrogen loading to test the influence of the pulse length of a short-pulse laser source. For each grating, the spectral width (FWHM) is recorded versus the reflection wavelength. As predicted by equation (12), the selection of a specific wavelength by tilting the mirrors affects the effective grating length and therefore the spectral width of the grating. Fig. 8 shows the reflection of two gratings. One grating reflects at the design wavelength of the phase mask (1030 nm) and has a reflection bandwidth of 3.3 nm, which reduces down to 1 nm for the other grating that reflects at 1111 nm. To show that such a reduction is caused by the effect of the grating length reducing with increasing mirror tilt $|\phi|$, we estimated the maximum bandwidth versus target wavelength using equation (12). This is represented by the solid line in Fig. 9. The flat region around 1030 nm is defined by the entrance slit of 1 cm, which corresponds to a maximum reflection bandwidth of 3.35 nm. Fiber Bragg gratings have been successfully inscribed for a wavelength range from 1030 to 1100 nm. The result in Fig. 9 shows that it is possible to inscribe chirped gratings over a wide spectral range with the same beam-splitting phase mask and a femtosecond laser source. The maximum spectral reflection bandwidth of the gratings is obtained in close proximity to the design Bragg reflection wavelength of the phase mask. We did not observe a reduction of the contrast in the interference pattern due to the spectral width of the applied laser. It is possible to expand the wavelength range of the PMI by further adjusting the geometry of the phase mask and the beam splitter [50].

IV. Conclusion

The chirped PMI has been shown to be suitable for the inscription of chirped fiber Bragg gratings with good wavelength versatility. Best results can be obtained when coherence properties of the applied laser system are taken into account. In this study, two laser systems with opposing coherence properties were investigated: an ultraviolet excimer and an ultraviolet femtosecond laser. With the excimer laser source, gratings were written from the visible spectral range up to the short-wave infrared range at 2000 nm. The bandwidth of the gratings increases with increasing Bragg reflection wavelength and reached values up to 10 nm. Chirped fiber Bragg gratings written with a single pulse demonstrate the potential for grating inscription even during the fiber drawing process. Wavelength versatility was also shown with the DUV femtosecond laser with a reduced wavelength range compared to the excimer laser source. This is related to the pulse length of the inscription laser. We believe that inscription with the chirped PMI with femtosecond laser and excimer laser opens novel applications, such as resonator mirrors for fiber laser setups and special filters for biophotonic applications.

References

[1] F. Ouellette, "Dispersion cancellation using linearly chirped Bragg grating filters in optical waveguides," *Opt. Lett.*, vol. 12, no. 10, pp. 847–849, 1987.
[2] M. C. Farries, C. M. Ragdale, and D. C. J. Reid, "Broadband chirped fibre Bragg filters for pump rejection and recycling in erbium doped fiber amplifiers," *Electron. Lett.*, vol. 28, pp. 487–489, 1992.
[3] P. A. Morton, V. Mizrahi, P. A. Andrekson, T. Tanbun-Ek, R. A. Logan, P. Lemaire, D. L. Coblentz, A. M. Sergent, K. W. Wecht, and P. F. Sciortino Jr, "Mode-locked hybrid soliton pulse source with extremely wide operating frequency range," *IEEE Photon. Technol. Lett.*, vol. 5, no. 1, pp. 28–31, Feb. 1993.
[4] F. Trepanier, G. Brochu, M. Morin, and A. Mailloux, "High-end FBG design and manufacturing for industrial lasers, sensing and telecommunications," presented at the Bragg Gratings, Photosensitivity, and Poling in Glass Waveguides, Barcelona, Spain, 2014, p. BM4D.1.
[5] P. J. Russell, J. L. Archambault, and L. Reekie, "Fiber gratings," *Phys. World*, pp. 41–48, 1993.
[6] W. Xie, M. Douay, P. Bernage, P. Niay, J. Bayon, and T. Georges, "Second order diffraction efficiency of Bragg gratings written within germanosilicate fibres," *Opt. Commun.*, vol. 101, pp. 85–91, 1993.
[7] O. Prakash, R. Mahakud, S. Dixit, and U. Nundy, "Effect of the spatial coherence of ultraviolet radiation (255 nm) on the fabrication efficiency of phase mask based fiber Bragg gratings," *Opt. Commun.*, vol. 263, no. 1, pp. 65–70, 2006.
[8] R. Mahakud, O. Prakash, J. Kumar, S. V. Nakhe, and S. K. Dixit, "Analysis on the effect of UV beam intensity profile on the refractive index modulation in phase mask based fiber Bragg grating writing," *Opt. Commun.*, vol. 285, no. 24, pp. 5351–5358, 2012.

[9] R. Kashyap, P. McKee, R. Campbell, and D. Williams, "Novel method of producing all fibre photoinduced chirped gratings," *Electron. Lett.*, vol. 30, no. 12, pp. 996–998, 1994.

[10] R. Kashyap, H.-G. Froehlich, A. Swanton, and D. Armes, "1.3 m long super-step-chirped fibre Bragg grating with a continuous delay of 13.5 ns and bandwidth 10 nm for broadband dispersion compensation," *Electron. Lett.*, vol. 32, no. 19, pp. 1307–1309, 1996.

[11] M. Melo and P. V. S. Marques, "Fabrication of tailored Bragg gratings by the phase mask dithering/moving technique," *Photon. Sensors*, vol. 3, no. 1, pp. 81–96, 2013.

[12] Y. Painchaud, A. Chandonnet, and J. Lauzon, "Chirped fibre gratings produced by tilting the fibre," *Electron. Lett.*, vol. 31, no. 3, pp. 171–172, 1995.

[13] K. C. Byron, K. Sugden, T. Bricheno, and I. Bennion, "Fabrication of chirped Bragg gratings in photosensitive fibre," *Electron. Lett.*, vol. 29, no. 18, pp. 1659–1660, 1993.

[14] L. Dong, J. Cruz, L. Reekie, and J. Tucknott, "Fabrication of chirped fibre gratings using etched tapers," *Electron. Lett.*, vol. 31, no. 11, pp. 908–909, 1995.

[15] J. L. Cruz, L. Dong, S. Barcelos, and L. Reekie, "Fiber Bragg gratings with various chirp profiles made in etched tapers," *Appl. Opt.*, vol. 35, no. 34, pp. 6781–6787, 1996.

[16] K. Sugden, I. Bennion, A. Molony, and N. Copner, "Chirped gratings produced in photosensitive optical fibres by fibre deformation during exposure," *Electron. Lett.*, vol. 30, no. 5, pp. 440–441, 1994.

[17] K. Byron and H. Rourke, "Fabrication of chirped fibre gratings by novel stretch and write technique," *Electron. Lett.*, vol. 31, no. 1, pp. 60–61, 1995.

[18] A. Asseh, H. Storoy, B. E. Sahlgren, S. Sandgren, and R. A. H. Stubbe, "A writing technique for long fiber Bragg gratings with complex reflectivity profiles," *J. Lightw. Technol.*, vol. 15, no. 8, pp. 1419–1423, Aug. 1997.

[19] G. Emmerson, S. Watts, C. Gawith, V. Albanis, M. Ibsen, R. Williams, and P. Smith, "Fabrication of directly UV-written channel waveguides with simultaneously defined integral Bragg gratings," *Electron. Lett.*, vol. 38, no. 24, pp. 1531–1532, 2002.

[20] I. Petermann, B. Sahlgren, S. Helmfrid, A. T. Friberg, and P.-Y. Fonjallaz, "Fabrication of advanced fiber Bragg gratings by use of sequential writing with a continuous-wave ultraviolet laser source," *Appl. Opt.*, vol. 41, no. 6, pp. 1051–1056, 2002.

[21] M. Gagné, L. Bojor, R. Maciejko, and R. Kashyap, "Novel custom fiber Bragg grating fabrication technique based on push-pull phase shifting interferometry," *Opt. Exp.*, vol. 16, no. 26, pp. 21 550–21 557, 2008.

[22] K. M. Chung, L. Dong, C. Lu, and H. Y. Tam, "Novel fiber Bragg grating fabrication system for long gratings with independent apodization and with local phase and wavelength control," *Opt Exp.*, vol. 19, no. 13, pp. 12 664–12 672, 2011.

[23] C. Knothe and E. Brinkmeyer, "Reset-free phase shifter in a Sagnac-type interferometer for control of chirp and apodization of Bragg gratings," presented at the Conf. Bragg Gratings, Photosensitivity Poling Glass Waveguides, Monterey, CA, USA, 2003, p. TuB3.

[24] C. Knothe, *Holographisches Herstellungsverfahren für Bragg-Gitter in UV-sensitiven Wellenleitern (german)*. Dusseldorf, Germany: VDI Verlag GmbH, 2005.

[25] M. Farries, K. Sugden, D. Reid, I. Bennion, A. Molony, and M. Goodwin, "Very broad reflection bandwidth (44 nm) chirped fibre gratings and narrow bandpass filters produced by the use of an amplitude mask," *Electron. Lett.*, vol. 31, no. 11, pp. 891–892, 1994.

[26] D. D. Garchev, M. Vasiliev, and D. J. Booth, "Wavelength-tunable chirped in-fiber Bragg gratings produced with a prism interferometer," *Opt. Commun.*, vol. 147, nos. 4–6, pp. 254–258, 1998.

[27] A. Dragomir, D. N. Nikogosyan, K. A. Zagorulko, P. G. Kryukov, and E. M. Dianov, "Inscription of fiber Bragg gratings by ultraviolet femtosecond radiation," *Opt. Lett.*, vol. 28, no. 22, pp. 2171–2173, 2003.

[28] S. J. Mihailov, C. W. Smelser, P. Lu, R. B. Walker, D. Grobnic, H. Ding, G. Henderson, and J. Unruh, "Fiber Bragg gratings made with a phase mask and 800-nm femtosecond radiation," *Opt. Lett.*, vol. 28, no. 12, pp. 995–997, 2003.

[29] M. Bernier, Y. Sheng, and R. Vallée, "Ultrabroadband fiber Bragg gratings written with a highly chirped phase mask and infrared femtosecond pulses." *Opt Exp.*, vol. 17, no. 5, pp. 3285–3290, 2009.

[30] J. Thomas, C. Voigtländer, D. Schimpf, F. Stutzki, E. Wikszak, J. Limpert, S. Nolte, and A. Tünnermann, "Continuously chirped fiber Bragg gratings by femtosecond laser structuring," *Opt. Lett.*, vol. 33, no. 14, pp. 1560–1562, 2008.

[31] C. Voigtländer, R. G. Becker, J. Thomas, D. Richter, A. Singh, A. Tünnermann, and S. Nolte, "Ultrashort pulse inscription of tailored fiber Bragg gratings with a phase mask and a deformed wavefront," *Opt. Mater. Exp.*, vol. 1, no. 4, pp. 633–642, 2011.

[32] C. Voigtländer, J. Thomas, E. Wikszak, P. Dannberg, S. Nolte, and A. Tünnermann, "Chirped fiber Bragg gratings written with ultrashort pulses and a tunable phase mask," *Opt. Lett.*, vol. 34, no. 12, pp. 1888–1890, 2009.

[33] G. D. Marshall, R. J. Williams, N. Jovanovic, M. J. Steel, and M. J. Withford, "Point-by-point written fiber-Bragg gratings and their application in complex grating designs," *Opt Exp.*, vol. 18, no. 19, pp. 19 844–19 859, 2010.

[34] R. Kashyap, "Assessment of tuning the wavelength of chirped and unchirped fibre Bragg grating with single phase-masks," *Electron. Lett.*, vol. 34, no. 21, pp. 2025–2027, 1998.

[35] M. L. Dockney, S. W. James, and R. P. Tatam, "Fibre Bragg gratings fabricated using a wavelength tuneable laser source and a phase mask based interferometer," *Meas. Sci. Technol.*, vol. 7, pp. 445–448, 1996.

[36] S. Pissadakis and L. Reekie, "An elliptical Talbot interferometer for fiber Bragg grating fabrication," *Rev. Sci. Instrum.*, vol. 76, pp. 066101-1–066101-3, 2005.

[37] M. Becker, J. Bergmann, S. Brückner, M. Franke, E. Lindner, M. Rothhardt, and H. Bartelt, "Fiber Bragg grating inscription combining DUV sub-picosecond laser pulses and two-beam interferometry," *Opt. Exp.*, vol. 16, no. 25, pp. 19 169–19 178, 2008.

[38] A. Saliminia, A. Proulx, and R. Vallée, "Inscription of strong Bragg gratings in pure silica photonic crystal fibers using UV femtosecond laser pulses," *Opt. Commun.*, vol. 333, pp. 133–138, 2014.

[39] C. G. Askins, M. A. Putnam, G. M. Williams, and E. J. Friebele, "Stepped-wavelength optical-fiber Bragg grating arrays fabricated in line on a draw tower," *Opt. Lett.*, vol. 19, no. 2, pp. 147–149, 1994.

[40] C. Chojetzki, M. Rothhardt, J. Ommer, S. Unger, K. Schuster, and H.-R. Mueller, "High-reflectivity draw-tower fiber Bragg gratings—Arrays and single gratings of type II," *Opt. Eng.*, vol. 44, no. 6, pp. 06 0503-1–060 503-2, 2005.

[41] C. W. Smelser, S. J. Mihailov, D. Grobnic, P. Lu, R. B. Walker, H. Ding, and X. Dai, "Multiple-beam interference patterns in optical fiber generated with ultrafast pulses and a phase mask," *Opt. Lett.*, vol. 29, no. 13, pp. 1458–1460, 2004.

[42] C. M. Rollinson, S. A. Wade, B. P. Kouskousis, D. J. Kitcher, G. W. Baxter, and S. F. Collins, "Variations of the growth of harmonic reflections in fiber Bragg gratings fabricated using phase masks," *J. Opt. Soc. Amer. A*, vol. 29, no. 7, pp. 1259–1268, 2012.

[43] E. Brinkmeyer, *Optische Kommunikationstechnik (german)*. Berlin, Germany: Springer, 2002, ch. 12.9, pp. 428–441.

[44] R. Kashyap, S. V. Chernikov, P. F. McKee, and J. R. Taylor, "30 ps chromatic dispersion compensation of 400 fs pulses at 100 Gbits/s in optical fibres using an all fibre photoinduced chirped reflection grating," *Electron. Lett.*, vol. 30, no. 13, pp. 1078–1080, 1994.

[45] T. Erdogan and J. E. Sipe, "Tilted fiber phase gratings," *J. Opt. Soc. Amer. A*, vol. 13, no. 2, pp. 296–313, 1996.

[46] M. Rothhardt, V. Hagemann, R. Poehlmann, S. Schroeter, and H.-J. Fuchs, "Characterization of chirped phase masks for UV-applications by writing and investigation of fiber Bragg gratings," *Proc. SPIE*, vol. 3099, pp. 231–236, 1997.

[47] P. J. Lemaire, R. M. Atkins, V. Mizrahi, and W. A. Reed, "High pressure H_2 loading as a technique for achieving ultrahigh UV photosensitivity and thermal sensitivity in GeO_2 doped optical fibres," *Electron. Lett.*, vol. 29, no. 13, pp. 1191–1193, 1993.

[48] T. A. Nguty and R. J. Potton, "Photochemical changes in hydrogen-loaded optical fibres with application to Bragg grating formation," *Meas. Sci. Technol.*, vol. 8, p. 1055–1058, 1997.

[49] I. Ota, T. Tsuda, A. Shinozaki, S. Yodo, T. Ota, T. Shigematsu, and Y. Ibusuki, "Development of optical fiber gratings for WDM systems," *Furukawa Rev.*, vol. 19, pp. 35–40, 2000.

[50] M. Becker, T. Elsmann, A. Schwuchow, M. Rothhardt, S. Dochow, and H. Bartelt, "Fiber Bragg gratings in the visible spectral range with ultraviolet femtosecond laser inscription," *IEEE Photon. Technol. Lett.*, vol. 26, no. 16, pp. 1653–1656, Aug. 2014.

Authors' biographies not available at the time of publication.